Climate Dynamics
https://doi.org/10.1007/s00382-024-07192-4

ORIGINAL ARTICLE

Improving land surface feedbacks to the atmosphere in convection-permitting climate simulations for Europe

Kate Halladay[1] · **Ségolène Berthou**[2] · **Elizabeth Kendon**[1]

Received: 16 January 2023 / Accepted: 11 March 2024

Abstract
We investigated positive temperature (warm) and negative precipitation (dry) biases in convection-permitting model (CPM) simulations for Europe (2.2 km grid spacing) that were considerably larger than in equivalent regional climate model (RCM) simulations (12 km grid spacing). We found that improvements in dry biases could be made by (1) using a more complex runoff scheme which takes into account topography and groundwater, (2) delaying the onset of water stress in vegetation to enhance transpiration, (3) changing the microphysics scheme to CASIM (Cloud AeroSol Interacting Microphysics) which also decreases heavy rainfall and increases light rainfall. Increasing soil moisture to the critical point can remove dry precipitation biases in southern Europe but not in northern areas, indicating that soil moisture limitation is a key contributor to precipitation biases in the south only. Instead, in the north, changing the cloud scheme of the model has more impact on precipitation biases. We found that the more intense and intermittent nature of rainfall in the CPM, which is more realistic leads to different canopy interception compared to the RCM. This can impact canopy evaporation, evapotranspiration and feed back on precipitation. Increasing rainfall storage in the canopy only leads to small improvements in warm biases, since it still fills rapidly with intense CPM rainfall, suggesting the need for an additional moisture store via improved groundwater modelling or surface pooling. Overall, this work highlights the challenge of correctly capturing land surface feedbacks in CPMs, which play an important role in future climate projections in some regions.

Keywords Convection-permitting climate models · Land-atmosphere interactions · Unified model · Europe

1 Introduction

Global circulation models (GCMs) and Regional Climate Models (RCMs) used in multi-model ensembles to inform climate policy decisions still use fully parametrised convection owing to their relatively coarse spatial resolution (approximately 1 degree in CMIP6). Convection-permitting models (CPMs) with typically < 5 km horizontal resolution, have been used for a number of years in weather forecasting but are increasingly applied on climate timescales, at least at the regional scale (e.g. Kendon et al. 2021). One of the key benefits of CPMs is an improved precipitation distribution compared to observations, i.e. less persistent, extensive light precipitation and more heavy precipitation. Several authors have noted that the change from convection-parametrised to convection-permitting models also affects land-surface interactions (e.g. Hohenegger et al. 2009, Leutwyler et al. 2021, Folwell et al. 2022). Such interactions become increasingly important when moving from weather to climate timescales, especially in seasonally dry regions, where soil moisture becomes the primary moisture source for evaporation during dry periods (e.g. Guo et al. 2006; Denissen et al. 2020). Observational studies have demonstrated the importance of soil moisture in convective organisation, initiation and intensification (e.g. Guillod et al. 2015; Klein and Taylor 2020). Errors in moisture fluxes between the atmosphere and the soil can become large on longer timescales and lead to biases that impact atmospheric processes. Therefore, an increased understanding of land/atmosphere interactions in CPMs is needed to ensure that they are appropriate for use in climate projections.

The land surface scheme exerts a control on the amount of rainfall intercepted by vegetation, so-called canopy

✉ Kate Halladay
kate.halladay@metoffice.gov.uk

[1] Met Office Hadley Centre for Climate Science and Services, Exeter, UK

[2] Met Office, Exeter, UK

Published online: 23 April 2024

interception, and the amount that reaches the surface either directly or by falling through the canopy (throughfall). This partitioning depends on rainfall rate. The land surface scheme and rainfall rate also control the amount of rain that infiltrates the soil column or contributes to runoff. Evaporation can occur either from the smaller canopy store or the large soil moisture store, either directly from the soil or through transpiration. Folwell et al. (2022) showed that in convection-permitting simulations for Africa (CP4 Africa, Stratton et al. 2018), the improved precipitation intensity distribution was accompanied by decreased canopy interception, decreased evapotranspiration (ET) and increased runoff. Similar results were also found over South America (Halladay et al. 2023). The more intense and intermittent nature of rainfall in the CPM reduces the efficiency of canopy interception. Folwell et al. (2022) also highlighted the role of the subgrid rainfall parametrisation[1] in addition to the precipitation intensity distribution in determining the partitioning of rainfall into canopy interception, infiltration into the soil and runoff and showed how these differences can feed back to the atmosphere.

Berthou et al. (2020) suggested that the treatment of soil hydraulics and runoff may be associated with summer warm and dry precipitation biases over Europe in 2.2 km CPM climate simulations with the Met Office Unified Model (UM). The dry biases were greater in 2.2 km CPM simulations than in similar 12 km RCM simulations with parametrised convection. We aim to understand why the summer (June-July-August) dry precipitation bias is greater in the CPM simulations compared to the 12 km RCM simulations. We also investigate the sensitivity of the warm and dry biases to different aspects of the land surface scheme using the Met Office UM at the same version as Berthou et al. (2020) (version 10.1, hereafter UM10.1-original) and in newer versions with the RAL3 (Regional Atmosphere Land 3) configuration (Bush et al. in prep.) and test model developments that could potentially reduce biases. Although this analysis is for the UM, we anticipate these sensitivities will apply to other CPMs. We examine the following potential causes of the warm/dry bias:

1. ET/latent heat flux from land to atmosphere is too low, thus limiting precipitation. This could be caused by
   (a) limited or low soil moisture/water availability, or
   (b) low canopy capacity, which may limit canopy evaporation and total evaporation. It was suggested by Davies-Barnard et al. (2014) that the canopy store is too small in the model. This meant that the excessive drizzle found in low-resolution, convection-parametrised models led to the canopy store constantly being refilled making canopy evaporation too high. They suggest that improvements in the precipitation intensity distribution brought by CPMs, i.e. decreased drizzle and increased heavy precipitation, may allow the canopy capacity to be increased to more realistic values.
2. atmospheric factors. If land surface factors can be excluded then it is likely that the warm/dry biases are associated with the atmosphere. If moisture flux to the atmosphere (ET) is already comparable with observations or greater, it is likely that atmospheric processes are limiting the formation of precipitation in some way, e.g. the atmospheric stability is too high so that convection is limited, convection is not initiating frequently enough, there are changes in cloud radiative effect, circulation patterns are biased leading to insufficient horizontal moisture convergence. The testing of these factors is largely outside the scope of this study but experiments are performed in which the microphysics and cloud schemes are changed.

Ultimately, we aim to find a 2.2 km CPM configuration of the UM that provides an improved representation of the present-day European climate (at least in terms of 1.5 m temperature and precipitation, and relative to the 12 km RCM) that can be used in climate-length, GCM-driven future simulations for Europe and potentially for other regions. First, we explore biases in ET in the CPMs and how they are related to dry/warm biases, breaking down ET into its canopy and soil components, building on work by Folwell et al. (2022) and Halladay et al. (2023). We test the impact on ET of increasing the capacity of the canopy store in line with observations and how this interacts with the different precipitation intensity distribution in CPMs. We also test the impact of changing the runoff scheme, soil properties and delayed onset of moisture stress in vegetation. Further we assess whether ET (and precipitation) can be increased by artificially removing soil moisture deficits, giving an indication of the contribution of soil moisture limitation to precipitation biases. Finally, we test the impact of changing the microphysics and cloud schemes.

Section 2 describes the model, differences between UM10.1-original and RAL3 and the setup of the various sensitivity tests. Section 3 describes and discusses the results including differences between standard model configurations, sensitivity tests, and their impact on biases. Summary and conclusions follow in Sect. 4.

[1] The aim of the subgrid rainfall parametrisation is to account for the non-uniform distribution of rainfall within a gridbox.

2 Model description and methods

2.1 Model description and experimental setup

The UM10.1-original configuration and domain including the JULES (Joint UK Land Environment Simulator) land surface scheme are described in Berthou et al. (2020). The 2.2 km CPM experiments in this analysis use the same pan-European domain (1536×1536 points, 70 vertical levels) with rotated pole and are directly downscaled (i.e. with no intermediate nest) from ERA-Interim[2] with 6-hourly lateral boundary conditions and daily SSTs from Reynolds et al. (2007). Other UM10.1 and Regional Atmosphere-Land 3 (RAL3) simulations start from 1st September 1998 and are initialised with the atmospheric and land surface state from the UM10.1-original simulation with that date. We performed simulations with standard configurations: UM10.1-original, RAL3-package 1 (hereafter RAL3-p1) and RAL3-package 3 (hereafter RAL3-p3) and a 12 km RCM for which we have 6 years of data (1999 to 2004). We also performed sensitivity tests with the CPMs based on standard configurations, which are five (2000 to 2004) or three years (1999 to 2001) in length. The details of the simulations with standard configurations and the sensitivity tests are listed in Table 1.

This section describes the key differences between the UM10.1-original and the RAL3 configurations used in our analysis. Section 2.1.1 describes the GL-RL (Global Land – Regional Land) consolidation package changes, and the following sub-sections describe changes to the atmospheric

Table 1 Configuration of experiments with the 2.2 km convection-permitting model and 12 km RCM with parameterised convection. PDM = Probability Distributed Model, p0 is a parameter related to soil moisture stress in vegetation (Sect. 2.1.1), LAI = leaf area index, plant functional types are: broadleaf tree, needleleaf tree, C3 grass, C4 grass, shrub. * indicates the latest UM configuration

Short name	Horiz. res.(km)	Analysis period	Cloud scheme	Microphysics scheme	Runoff scheme, excess soil moisture, soil hydraulic scheme	p0	Irrigation	Rate of change of canopy capacity with LAI (for each plant functional type)	notes
	Standard configurations								
UM10.1	2.2	1999–2004	Smith	Wilson & Ballard	PDM, up, van Genuchten	0	no	0.05, 0.05, 0.05, 0.05, 0.05	UM10.1-original configuration
RAL3-p1	2.2	1999–2004	bimodal	Wilson & Ballard	TOPMODEL, down, Brooks-Corey	0.6	no	0.05, 0.05, 0.05, 0.05, 0.05	RAL3-p1: includes a number of differences from UM10.1
RAL3-p3	2.2	1999–2004	bimodal	CASIM	TOPMODEL, down, Brooks-Corey	0.6	no	0.05, 0.05, 0.05, 0.05, 0.05	*RAL3-p3 with CASIM
RCM	12	1999–2004	PC2	Wilson & Ballard	TOPMODEL, down, Brooks-Corey	0	no	0.05, 0.05, 0.05, 0.05, 0.05	RCM
	Sensitivity tests (3- and 5-year)								
UM10.1 TOP	2.2	2000–2004	Smith	Wilson & Ballard	TOPMODEL, down, Brooks-Corey	0	no	0.05, 0.05, 0.05, 0.05, 0.05	UM10.1 with TOPMODEL
RAL3-p1 cncpmx	2.2	1999–2001	bimodal	Wilson & Ballard	TOPMODEL, down, Brooks-Corey	0.6	no	0.44,1.05, 0.95,1.375,1.5	RAL3-p1 with increased canopy capacity
RAL3-p1 irrig	2.2	1999–2001	bimodal	Wilson & Ballard	TOPMODEL, down, Brooks-Corey	0.6	yes	0.05, 0.05, 0.05, 0.05, 0.05	RAL3-p1 with irrigation: i.e. no soil moisture limitation
RAL3-p1 p0 = 0	2.2	1999–2004	bimodal	Wilson & Ballard	TOPMODEL, down, Brooks-Corey	0.0	no	0.05, 0.05, 0.05, 0.05, 0.05	RAL3-p1 no p0 change (i.e. original threshold for moisture stress in vegetation)
RAL3-p1 no bimod	2.2	1999–2004	Smith	Wilson & Ballard	TOPMODEL, down, Brooks-Corey	0.6	no	0.05, 0.05, 0.05, 0.05, 0.05	RAL3-p1 no bimodal cloud
RAL3-p3 cncpmx	2.2	1999–2001	bimodal	CASIM	TOPMODEL, down, Brooks-Corey	0.6	no	0.05, 0.05, 0.05, 0.05, 0.05	RAL3-p3 with CASIM and increased canopy capacity

[2] The UM10.1 simulation 'original hindcast' was started before ERA5 was available and therefore the experiments are driven with boundary conditions from ERA-Interim. As we wanted to compare the effects of changing configuration, we did not want to add complexity by changing the driving data.

component of the UM. Note that the bimodal cloud scheme is included in RAL3-p1 and RAL3-p3 but CASIM microphysics is included in RAL3-p3 only.

2.1.1 Land surface scheme

Key land surface differences between UM10.1-original and RAL3 configurations are as follows:

- *Use of a more complex runoff scheme*. The configuration used for UM10.1-original included the PDM (Probability Distributed Model, Moore, 1985) scheme for modelling of saturation- excess runoff, which is produced when the soil is saturated. This scheme only considers soil moisture heterogeneity in the uppermost soil layer and does not represent the water table (Best et al. 2011). In other simulations the alternative TOPMODEL scheme (Gedney and Cox 2003) was used. This is a more complex scheme that takes into account the topography, calculates a water table depth and includes an extra soil layer in which there is an exponential decrease of saturated hydraulic conductivity with depth controlled by a decay constant. Although the water table can move vertically according to saturation levels in the soil column, there is no lateral flow of groundwater between gridboxes.
- *Excess soil moisture directed downwards as opposed to upwards.* The default setting in UM10.1-original is for excess water in a supersaturated soil layer to be directed upwards towards the surface to be incorporated into surface runoff. Alternatively, this can be set to direct excess moisture downwards to contribute to sub-surface runoff as is the default setting in RAL3. This setting would be expected to increase soil moisture in the lower layers.
- *Brooks and Corey as opposed to van Genuchten for soil hydraulic*s. Berthou et al. (2020) found that soil parameter sets used in these experiments were inconsistent with the van Genuchten scheme (van Genuchten 1980) resulting in infiltration rates for soil moisture that were too low. They found that improvements could be made by switching to Brooks-Corey (Brooks and Corey 1964), thus many of the subsequent sensitivity tests include this this scheme. Brooks-Corey is now the default soil hydraulic scheme used in the latest RAL configuration of the UM (RAL3).
- *Reduction of the threshold at which ET becomes soil-moisture limited*. Harper et al. (2021) suggest that vegetation is too responsive to moisture stress in JULES which can cause transpiration and hence ET to be too low. They recommend a change in the value of the parameter p0 which controls this response from the default value of 0 to 0.6. This parameter was introduced to delay the onset of moisture stress, i.e. the plant can continue transpiring at lower values of soil moisture. This would be expected to increase transpiration provided there is sufficient soil moisture availability. However, if soil moisture is exhausted then transpiration must decrease later in the summer season.
- *Rain fraction (i.e. fraction of gridbox covered by precipitation or ϵ_r) is passed from the microphysics scheme to the land surface*. In the UM, precipitation is assumed to be exponentially distributed within a gridbox to take account of subgrid heterogeneity (Best et al. 2011). Rain fraction controls the shape of the distribution and is used in the calculation of infiltration-excess runoff[3] and throughfall (see Eqs. 46 and 48 in Best et al. 2011). Hence it has an impact on the amount of moisture reaching the soil surface. Fractions of less than 1.0 mean less interception, less infiltration and more runoff for a given rainfall rate as the total gridbox rainfall is contained within a smaller area. Previously (pre- RAL3), rain fraction would have been set to 1.0 for all precipitation in a CPM as convective and large-scale rain are not separated. Rain fractions output from the microphysics scheme in UM10.1 and RAL3-p1 are close to 1.0 suggesting that the change from a default value of 1.0 to using actual values from the microphysics scheme will not significantly impact precipitation biases.
- *Soil properties are calculated using a new method*, in which the soil properties of the dominant soil type at a grid point are used as opposed to combining the soil properties from all the soil types present at that grid point. However, the soil properties are still based on the same soil data as described in Bush et al. (2020). This results in a map of soil properties that resemble real soil types as opposed to less realistic 'hybrid' types. The new critical points and wilting points are mostly reduced across the domain in RAL3, allowing vegetation to maintain transpiration in drier soils compared with UM10.1.
- *Land cover ancillary data is based on the European Space Agency Climate Change Initiative land cover data set* (Hartley et al. 2017) as opposed to the International Geosphere Biosphere Programme (IGBP) dataset (Loveland et al. 2000).
- Additional changes include adjustments to vegetation and thermal roughness lengths, and updated leaf area index values and canopy heights.

2.1.2 Bimodal cloud scheme

The bimodal cloud scheme (van Weverberg et al. 2021) replaces the Smith scheme (Smith 1990) in RAL3. The Smith scheme assumes a unimodal, symmetrical sub-grid probability distribution function to represent temperature

[3] Infiltration-excess runoff occurs when the rainfall rate exceeds the rate of infiltration into the soil column.

and humidity fluctuations. It has been shown that this cannot generally represent temperature and moisture variability especially in entrainment zones near the top of the boundary layer and tends to underestimate cloud cover (van Weverberg et al. 2021). The bimodal scheme includes two modes of variability (dry, warm, free-tropospheric and moist, mixed layer) to represent the different characteristics of air either side of entrainment zones to calculate cloud liquid water content and cloud fraction.

2.1.3 CASIM microphysics scheme

The CASIM (Cloud AeroSol Interacting Microphysics) scheme which is part of the RAL3-p3 configuration replaces the modified Wilson & Ballard scheme described in Bush et al. (2020). CASIM includes cloud ice as a hydrometeor species in addition to the 4 species used by Wilson & Ballard: cloud droplets, rain, snow and graupel. CASIM is also a double moment scheme in the UM in that it is able to predict droplet mass as well as number. This means that for a given mass of droplets, the number of droplets can vary, thus allowing a broader range of particle sizes which in turn affects the precipitation intensity distribution. In the test using RAL3-p3 performed here, the cloud droplet number is fixed at 50 per cm^3, but rain droplet number can still vary. Initial tests for other regions with the CASIM microphysics scheme show that it decreases the tendency of the CPM to produce too much heavy rainfall and provides more spatial coherence of convective cells (Field et al. 2023.). It also increases total precipitation amounts compared with RAL3-p1 (which does not use CASIM) over the UK (Bush et al., in prep.).

2.2 Sensitivity tests

A number of sensitivity tests were performed based on the standard configurations of the 2.2 km CPM, in order to test some of the changes in configuration between UM10.1 and RAL3 and to explore the response to very wet soil and to increasing the size of the canopy moisture store (Table 1). 'UM10.1 with TOPMODEL' (Table 1) is based on UM10.1-original but includes TOPMODEL as opposed to PDM, excess soil moisture is directed downwards and Brooks-Corey soil hydraulics are used as opposed to van Genuchten. The first year of this test (1999) was discarded as an error was found in the spin-up settings, which resulted in the soil being too wet during that year. Therefore, only the period 2000 to 2004 from this simulation is analysed. Two further tests based on RAL3-p1 exclude the p0 change (p0 = 0.0) and the bimodal cloud scheme (reverts to Smith scheme). Further sensitivity tests are described in the following sections.

2.2.1 RAL3-p1 with irrigation

One way to investigate whether dry precipitation biases are related to negative biases in soil moisture is to artificially add moisture to the soil in order to remove any soil moisture deficits and maximise transpiration and soil evaporation. If negative precipitation biases still exist then soil moisture limitation can be ruled out as a cause. Bastin et al. (2018) carried out a saturated soil experiment for Europe to investigate the degree to which soil moisture limited transpiration in summer. They found that in their model, the latent heat flux was still too low despite the removal of soil moisture limitation. The irrigation demand scheme has recently become available in the UM as opposed to just the land-surface model (JULES). This scheme adds water to the top two soil layers such that soil moisture does not drop below the critical point, thus avoiding soil moisture limitation of transpiration. This experiment is therefore similar to that performed by Bastin et at (2018). It aims to establish whether areas of negative ET bias in the 2.2 km simulations are caused by soil moisture limitation. Note that amount of added water is unlimited so that with time, the total soil moisture increases towards saturation. It is nonetheless useful to examine the effects on evapotranspiration for a limited period.

2.2.2 RAL3-p1 and RAL3-p3 with increased canopy capacity

Canopy capacity is defined as the amount of intercepted water that vegetation can hold. It is calculated for each plant functional type according to Eq. 15 from Best et al. (2011):

$$C_m = A_m + B_m L$$

where Cm is canopy capacity (kg m^{-2}), L is leaf area index (LAI) (m^2 m^{-2}), A_m is puddling of water on soil surface and interception by leafless vegetation (kg m^{-2}) and B_m is rate of change of water holding capacity with leaf area index (kg m^{-2}). A_m and B_m are tile-dependent parameters.

In these experiments, canopy capacity values were modified by changing the parameter 'Bm' (Table 2) so that the canopy capacity values matched maximum values listed for Europe in Table 8 in Breuer et al. (2003). The resulting canopy capacity values calculated with default LAI values are shown in Table 2. These values are intended as an unphysically large perturbation compared to the default values so that the signal can be maximised. The actual increases in canopy capacity for July with increased canopy capacity, calculated using the prescribed LAI values show some considerable spatial variability which is related to the plant functional type composition in each gridbox (Supplementary

Table 2 Default and Breuer et al. (2003) values of canopy capacity in mm (Cm) calculated from minimum canopy capacity (Am), rate of change of canopy capacity with LAI (Bm) and default LAI values for 5 plant functional types

		Broadleaf tree (leaf area index = 5)	Needleleaf tree (leaf area index = 4)	C3-grass (leaf area index = 2)	C4-grass (leaf area index = 4)	Shrub (leaf area index = 1)
Default	Am, Bm	0.5, 0.05	0.5, 0.05	0.5, 0.05	0.5, 0.05	0.5, 0.05
	Cm	**0.75**	**0.7**	**0.6**	**0.7**	**0.55**
Breuer Europe (max)	Am, Bm	0.5,0.44	0.5,1.05	0.5,0.95	0.5,1.375	0.5,1.5
	Cm	**2.7**	**4.7**	**2.4**	**6.0**	**2.0**

Figure 1). The same canopy capacity changes were applied to RAL3-p1 and RAL-p3 configurations to investigate the impact of canopy capacity changes with both Wilson and Ballard and CASIM microphysics schemes.

2.2.3 Additional sensitivity tests

In addition to the tests already described and listed in Table 1, sensitivity tests were performed to explore (1) changes in the land cover data, specifically increased grass and decreased bare soil fraction, (2) changes in the decay rate of saturated hydraulic conductivity with depth and maximum depth to the water table, (3) using soil properties based on the SoilGrids (Hengl et al. 2017) data set, (4) enhanced infiltration and (5) removing subgrid rainfall variability (Supplementary information).

2.3 Observational datasets

For the evaluation of precipitation and temperature biases for the 6 years over which RAL3-p1 can be compared with UM10.1 simulations at 2.2 and 12 km resolution, we have used E-OBS v20.0e as this covers the whole domain (Cornes et al. 2018). For precipitation, however, we also used the country- or region-specific datasets for France, Germany, UK and the Alps (including Switzerland, Austria, Slovenia, northern Italy and part of Croatia) that were used in Berthou et al. (2020), which cover a more limited area (Supplementary Figure 2). At the regional and monthly scale, we find minimal differences between the region-specific datasets and E-OBS for precipitation.

For evaluation of ET biases we used GLEAMv3.5a (Miralles et al. 2011; Martens et al. 2017). This data set uses a set of algorithms to estimate evapotranspiration and its components. Potential evaporation is calculated using the Priestly and Taylor equation, which is multiplied by output from the stress module combining observed precipitation and satellite-derived soil moisture. The result is then added to an estimated value of rainfall interception using the Gash analytical model to provide an estimation of evapotranspiration. The inputs to the algorithms come from a combination of reanalysis and satellite observations. For ET we also use the FluxCom data set (Jung et al. 2019). This data set includes energy flux measurements from eddy covariance towers combined with remote sensing inputs from MODIS satellites and global meteorological data to produce an ensemble of estimates using different machine-learning and energy balance closure methods.

3 Results and discussion

The first Sect. (3.1) explores biases in the standard configurations for the period 1999 to 2004. The subsequent sections discuss results from sensitivity tests, which are categorised as related to canopy, soil or atmospheric processes. For Figs. 1, 2, 3, 4, 5 and 6, sensitivity tests are grouped by duration (3 or 5 years) so that the relative impact of the tests can be compared for the same period.

3.1 Biases in precipitation, 1.5 m temp and ET for standard configurations

Berthou et al. (2020) described summer warm and dry biases in 2.2 km hindcast simulations for Europe using UM10.1-original (Figs. 1b and 2b). The dry precipitation bias is greater in some areas of western and central Europe in UM10.1-original (with explicit convection) compared with the 12 km RCM (with parametrised convection) (Fig. 1a and b). In Figs. 1 and 2 we also compare biases with respect to E-OBS in other more recent configurations of the UM. The areas where the dry precipitation bias is greater in the CPMs are mostly over France (up to around 50%) compared to a maximum of around 25% in the RCM. However, the root mean squared error (RMSE) value for the whole domain (excluding masked areas[4]) is highest in the 12 km RCM due to some areas of strong positive bias. Lowest RMSE values among CPM configurations are associated with RAL3-p3. The spatial patterns and relative magnitudes of precipitation bias are similar when using the region-specific datasets used in Berthou et al. (2020) (Supplementary Figure 2).

For temperature, there are widespread warm biases across central Europe of over 0.5 K and up to around 3 K towards

[4] Regions with mean precipitation of less than 1 mm/day are masked as the percentage changes in these areas can appear very large although absolute changes are very small.

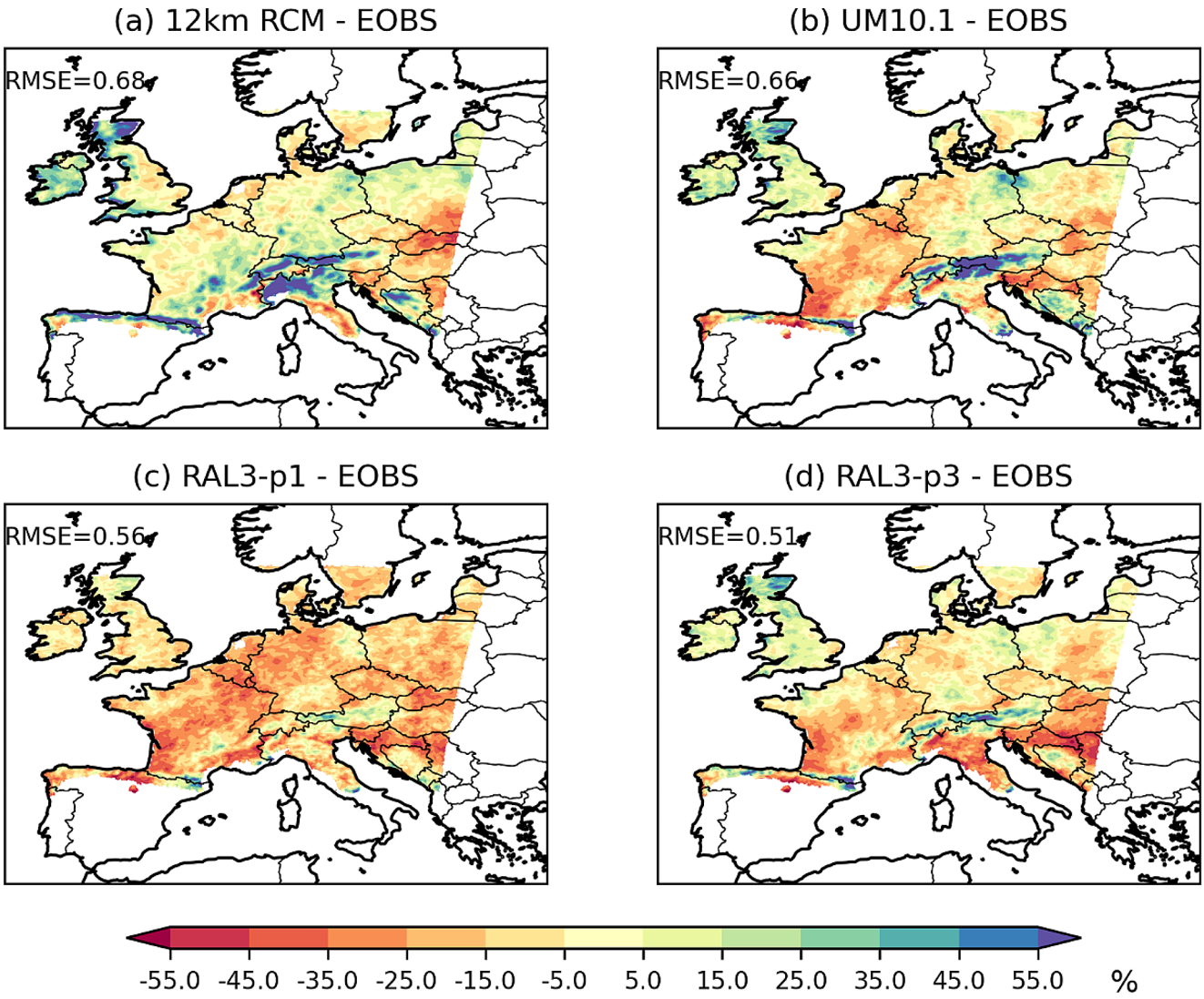

Fig. 1 June-July-August (JJA) percent precipitation bias 1999–2004 for standard configurations compared with observations from E-OBS for (a) 12 km RCM (b) UM10.1-original, (c) RAL3-p1, (d) RAL3-p3. Regions with mean precipitation of less than 1 mm per day during the period of evaluation are masked

the eastern edge of the domain (Fig. 2). The total RMSE for the domain is greater in UM10.1-original compared to the 12 km RCM and is lowest in RAL3-p3. A decrease in the warm bias between UM10.1-original and RAL3-p3 is also visible in the maps (Fig. 2b and d).

We note that the period of evaluation is relatively short, therefore, we have plotted precipitation and temperature biases for each year (Supplementary Figs. 3 and 4). For precipitation, there is some year to year variability in the sign of bias, e.g. over France in the 12 km RCM, though the dry bias at the eastern edge of the domain and the wet bias over the Alps are relatively consistent. In RAL3-p1 there are widespread dry biases each year, which are generally weaker in RAL3-p3. For 1.5 m temperature, there is more consistency in the location and sign of the bias from year to year.

Further investigation showed that there is also a difference in the ET bias between the 12 km and 2.2 km models. Comparisons with GLEAM suggest a positive ET bias over France, UK and Germany in the 12 km RCM, but negative biases over southern Europe (Fig. 3a). In UM10.1-original (Fig. 3b) there is a negative bias in all regions except the Alps and NE Germany. Given the uncertainty in gridded ET products, bias has also been calculated relative to the FluxCom data for 2001 to 2004 (Supplementary Figure 5). The spatial pattern of bias is similar to that of GLEAM, though negative biases in southern areas are greater (up to 2 mm/day in the southeast of the domain) and positive biases in the RCM and RAL3-p3 are close to zero or slightly negative. With both ET datasets, the greatest negative biases and highest RMSE values are in UM10.1-original and lowest RMSE values occur with the RCM.

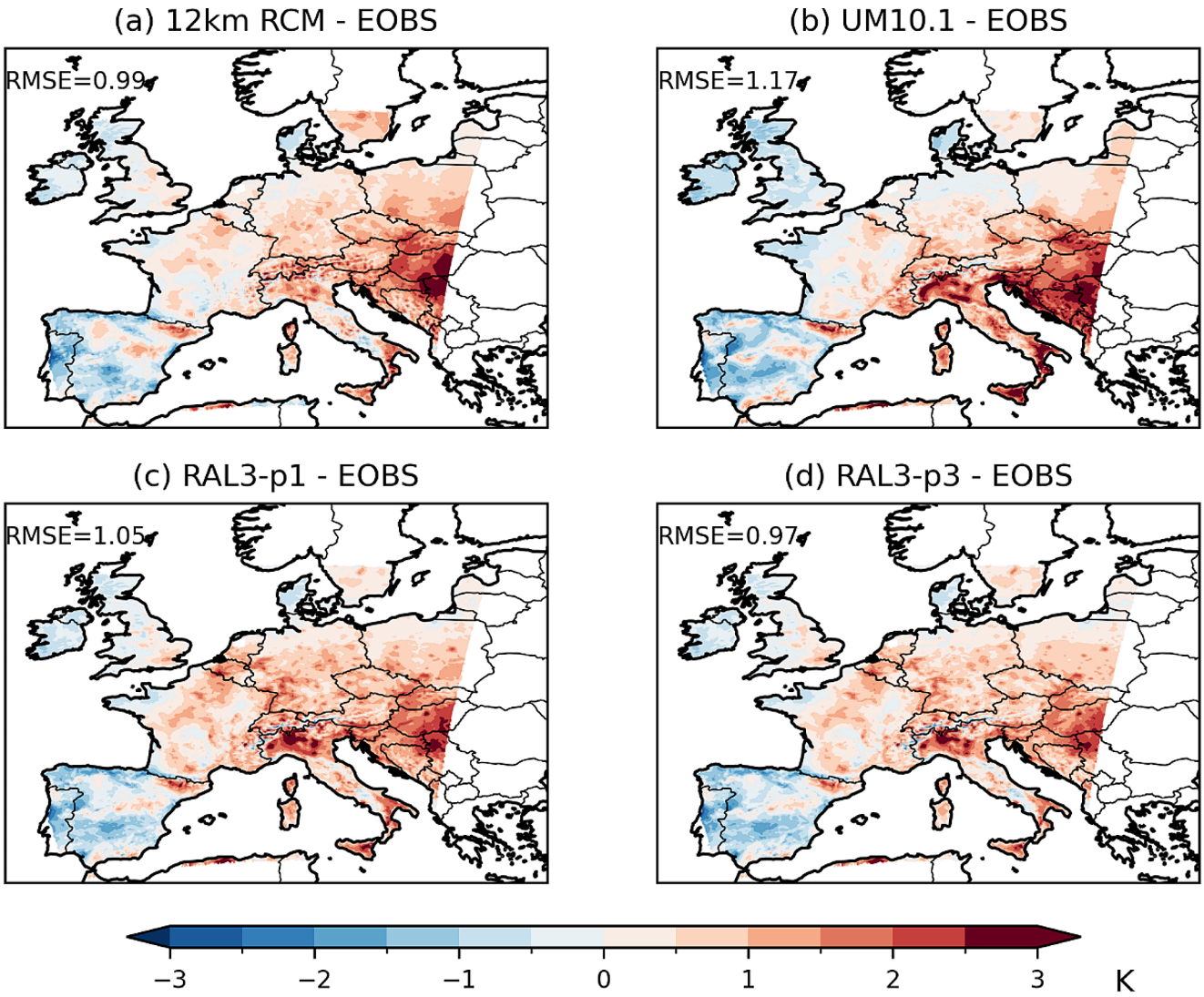

Fig. 2 JJA 1.5 m temperature bias (K) for standard configurations (1999–2004) compared with observations from EOBS for (a) 12 km RCM (b) UM10.1-original, (c) RAL3-p1, (d) RAL3-p3

3.2 Canopy processes

3.2.1 Understanding ET differences between the RCM and CPMs

Comparing annual cycles of monthly mean canopy evaporation and ET in the RCM and CPMs (standard configurations and 5-year sensitivity tests) averaged over France (Fig. 4) shows that in summer, ET and canopy evaporation are lower in the CPM simulations, indeed, canopy evaporation is consistently lower throughout the annual cycle. Canopy evaporation was also found to be lower in the CPM simulations throughout the annual cycle averaged over Spain, Germany and southern UK (not shown). The CPMs with the smallest difference in ET compared to the RCM are UM10.1 with TOPMODEL and RAL3-p3 (dashed red line and blue line in Fig. 4). The mean contribution to the ET[5] difference in UM10.1 with TOPMODEL is dominated by the difference in canopy evaporation as opposed to soil evaporation during most of the annual cycle except in June (Fig. 5). This may be because canopy evaporation requires canopy interception and rainfall, which is at a minimum in June (Fig. 4). Therefore, moisture for ET is derived predominantly from the soil and differences between RCM and CPM are larger in soil evaporation. Similar results were found for RAL3-p3 (not shown).

To understand the CPM/RCM difference in canopy evaporation, we investigated the effect of the precipitation intensity distribution (i.e. the relative contribution from heavy and

[5] Note that ET is approximately equal to the sum of soil evaporation (including bare soil evaporation and transpiration) and canopy evaporation.

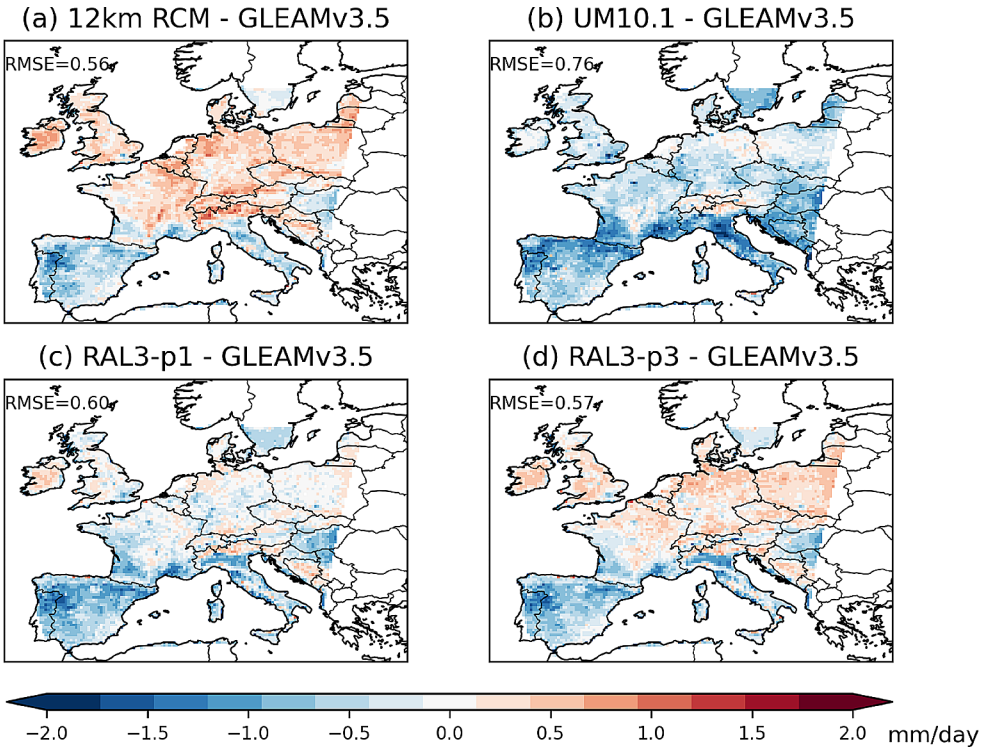

Fig. 3 ET bias for JJA (mm/day) for standard configurations compared with observations from GLEAM v3.5 (1999–2004) based on monthly mean data from (a) 12 km RCM, (b) UM10.1-original, (c) RAL3-p1, (d) RAL3-p3

light rainfall) on canopy evaporation using timestep (1 min) output. We identified precipitation events during summer 2000, which were defined as having a peak in precipitation rate of >0.05 mm/minute or 3 mm/hr. This threshold was chosen as it identified a manageable number of events. We find that when precipitation occurs, the canopy water content is often already at or close to its maximum level, so rainfall can no longer be intercepted and canopy evaporation cannot increase. Therefore, the intensity and intermittency of rainfall are key in determining the amount of rainfall that can be intercepted. Moreover, in summer when evaporation rates are high, ET is moisture-limited, and given that the canopy store is small (<1 mm based on default values), the intercepted water usually evaporates very quickly after rain. More intense and intermittent rainfall, as seen in the CPM compared to the RCM, results in a greater number of timesteps when the canopy water content is zero and there is no canopy evaporation, even though the total amount of precipitation may be similar. Other explanations were considered (see Supplementary information), however, our results suggest that changes in the precipitation intensity distribution (as shown by Berthou et al. 2020) affect the amount of canopy evaporation and hence ET. This is in agreement with the findings of Folwell et al. (2022) for CPM simulations over Africa. They showed that despite adjustments to the subgrid rainfall parametrisation of canopy interception in the RCM compared to the CPM, the canopy evaporation difference remained. The canopy store is so frequently refilled by light rainfall in the RCM compared to the CPM that it more than compensates for the adjustment.

The change in ET partitioning in the CPM can result in decreased ET, increased runoff and reduced coupling between land surface and atmosphere as shown for Africa in Folwell et al. (2022). Reduced coupling occurs when ET is too dependent on 'fast' storage such as the canopy store, which is quickly emptied and thus ET cannot be maintained in the summer without an adequate moisture source for transpiration. A low ratio of transpiration to total ET (i.e. too much canopy evaporation) was cited by Dong et al. (2022) as a cause of warm biases in the simulations for the central US.

3.2.2 Impact of increased canopy capacity

Artificially increasing the canopy capacity in the CPM results in widespread increases in canopy evaporation with both microphysics schemes in 3-year sensitivity tests (Fig. 6d and i). We note that regions of increased canopy evaporation are not entirely consistent with the areas of increased canopy capacity (Supplementary Figure 1), as canopy evaporation is also influenced by rainfall amount and intensity distribution. We also find that there is a lesser effect on ET than canopy evaporation (Fig. 6c and h) with most areas seeing a small increase. This indicates that most of the increase in canopy evaporation is balanced by a decrease in soil evaporation as opposed to increasing total ET. The effects on cloud fraction (Fig. 6e and j)

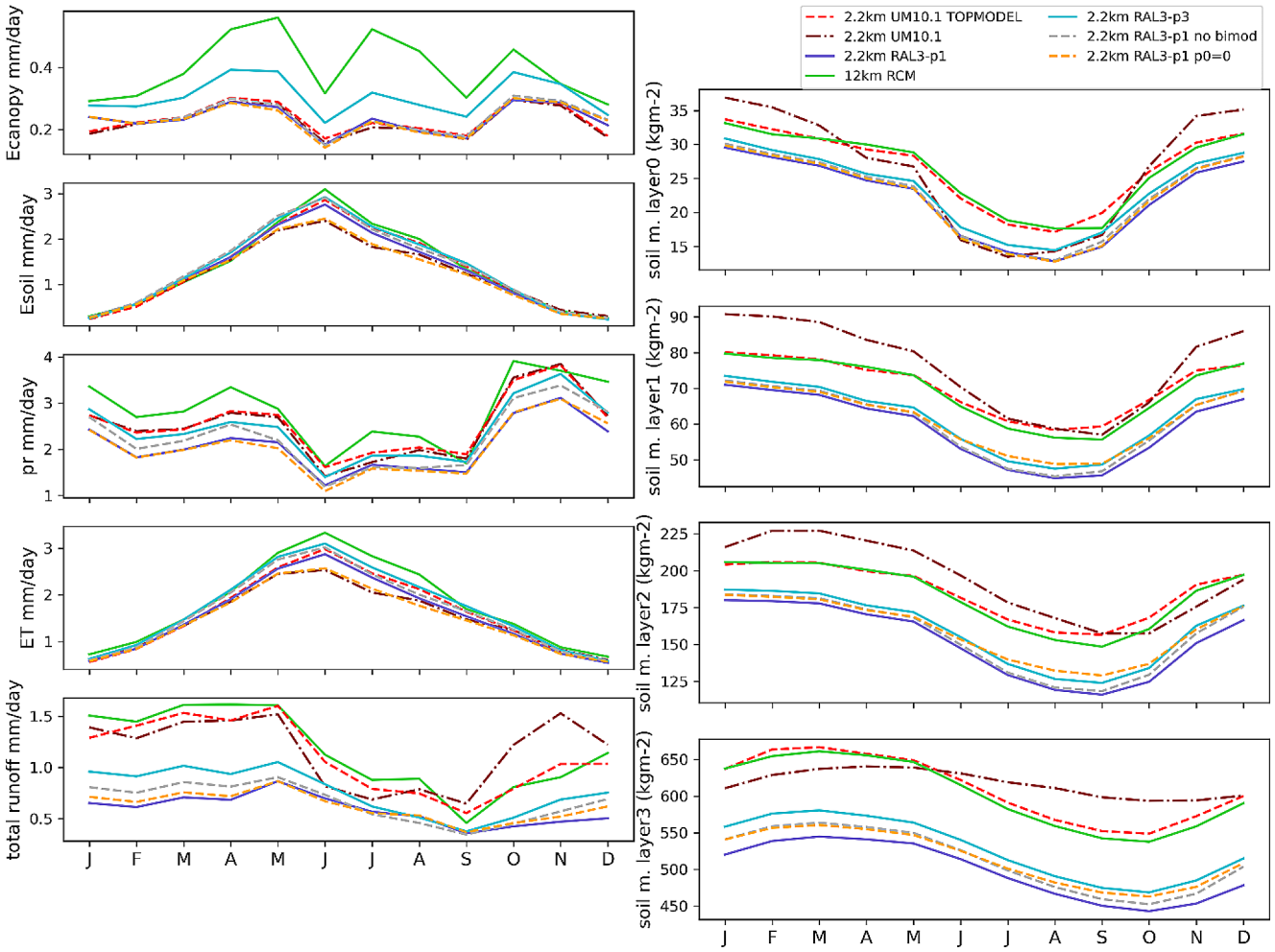

Fig. 4 Annual cycles of canopy evaporation, soil evaporation, precipitation, ET, total runoff and soil moisture content on each layer (2000–2004) in standard configurations: 12 km RCM, UM10.1-original, RAL3-p1, RAL3-p3 and 5-year sensitivity tests: UM10.1 with TOPMODEL, RAL3-p1 with p0 = 0, RAL3-p1 with no bimodal cloud averaged over France. Soil layer depths for layers 0 to 3 are 0.1, 0.25, 0.65 and 1.0 m, making a total depth of 3 m

and shortwave and longwave radiation at the surface are very small (Supplementary Figure 6a to d). In many areas, there is a cooling effect from increased canopy capacity of approximately 0.25 °C (Fig. 6b and g). In RAL3-p3 with increased canopy capacity there is slightly more widespread cooling effect and increased precipitation in some areas (Fig. 6f and g). This is accompanied by more negative net surface shortwave (SWnet) and more positive net surface longwave (LWnet) radiation (Supplementary Figure 6e,f).

We find that precipitation biases and RMSE are largely unchanged compared with RAL3-p1 (Supplementary Figure 7), however, the cooling effect slightly reduces the 1.5 m temperature bias and RMSE (Supplementary Figure 8b,d) for the same period compared with standard configurations (Supplementary Figure 8a,c). So despite large increases in canopy capacity, changes in ET and precipitation are small. This result is in agreement with Davies-Barnard et al. (2014) who also found that the sensitivity of precipitation and ET to the increase to be low as the canopy store is still far smaller than the soil moisture store. Although increasing canopy capacity can decrease warm biases in this region and is more consistent with observations, this contrasts with the result from Dong et al. (2022) which attributed warm biases to too much canopy evaporation relative to transpiration. Moreover, canopy evaporation in the CPM may already be consistent with observations (Folwell et al. 2022), though canopy evaporation observations are limited making true values are difficult to constrain. Therefore, it may not be appropriate to increase it further.

3.3 Soil processes

3.3.1 Impact of removing soil moisture deficits (irrigation)

The third 3-year sensitivity test involved removal of soil moisture limitation (irrigation experiment – Sect. 2.2.1).

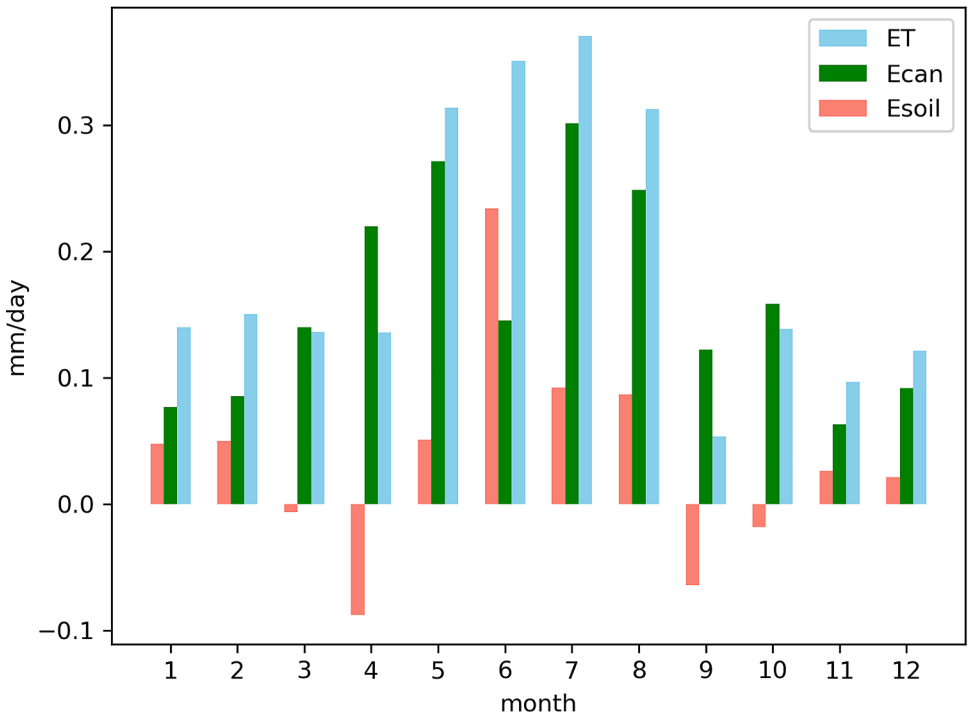

Fig. 5 Mean contribution to monthly mean ET difference between UM10.1 with TOP-MODEL and 12 km RCM from canopy evaporation (Ecan) and soil evaporation (Esoil) based on data from 2000 to 2004 averaged over France

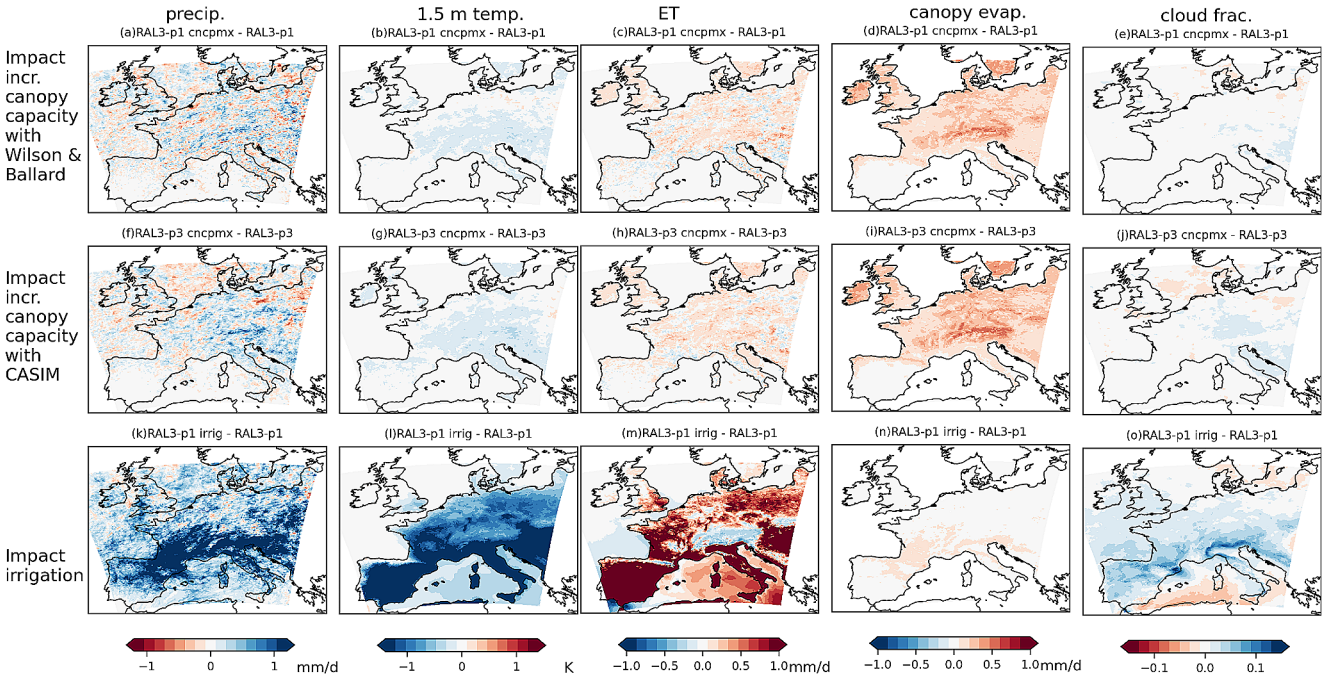

Fig. 6 Mean JJA difference (1999–2001) between standard RAL3 configurations and 3-year sensitivity tests. Top row: RAL3-p1 with increased canopy capacity, middle row: RAL3-p3 with increased canopy capacity and bottom row: RAL3-p1 with irrigation for (a),(f),(k) precipitation (mm/day), (b),(g),(l) 1.5 m temperature (K), (c),(h),(m) ET (mm/day), (d),(i),(n) canopy evaporation (mm/day) and (e),(j),(o) cloud fraction

This results in increases in precipitation of more than 1 mm/day in many areas (Fig. 6k) particularly across southern Europe, however, there are some areas in the north of the domain where dry precipitation biases persist (Fig. 7b). This suggests that the role of soil moisture and transpiration in generating rainfall is less important in northern areas than in southern Europe, and that increasing soil moisture in southern Europe could reduce dry precipitation biases via increases in ET. In the case of 1.5 m temperature (Fig. 6l), decreases in excess of 1 °C are evident in southern Europe

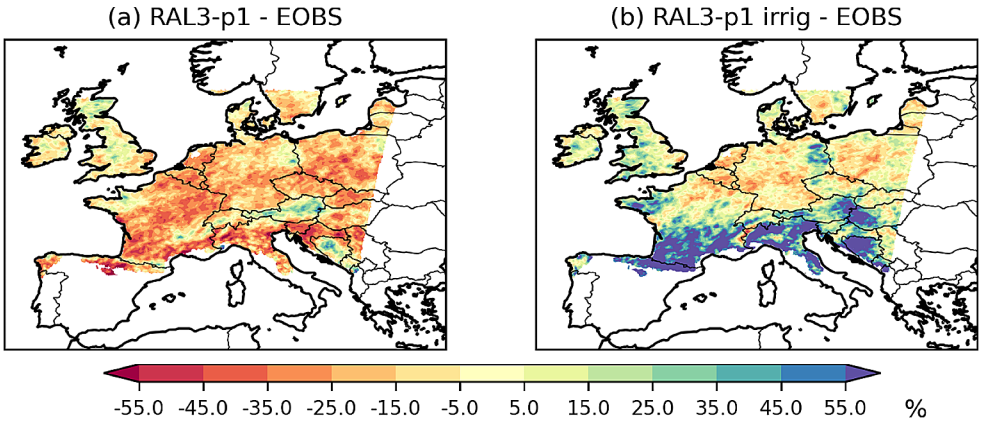

Fig. 7 Mean JJA precipitation bias (%) for 1999 to 2001 in (a) RAL3-p1 and (b) RAL3-p1 with irrigation compared with E-OBS. Regions with mean precipitaion of less than 1 mm per day during the period of evaluation are masked

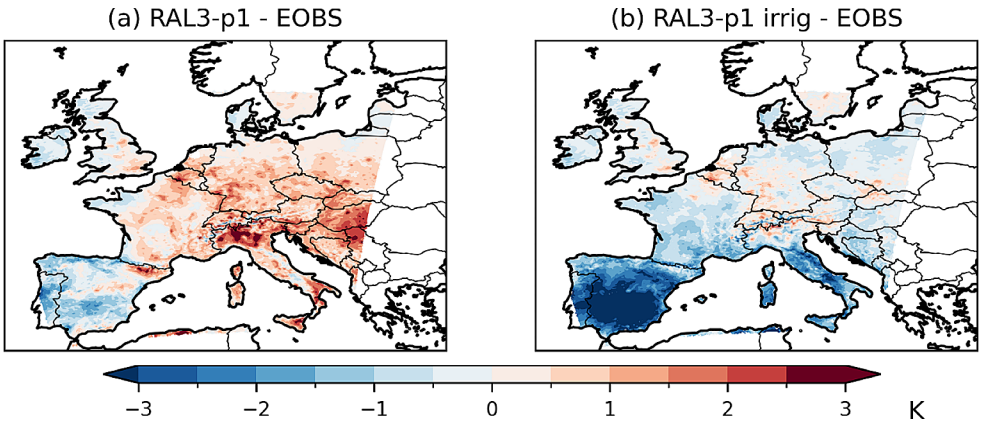

Fig. 8 Mean JJA 1.5 m temperature bias (K) for 1999 to 2001 in (a) RAL3-p1 and (b) RAL3-p1 with irrigation compared with E-OBS

and cooling occurs almost everywhere, as 1.5 m temperature is modified through increases in latent heat at the expense of sensible heat. Despite this, there are still areas of warm bias in central Europe (Fig. 8b). This may relate to the pattern of ET change in this test (Fig. 6m). ET changes are negative in some regions, notably the Alps. This could be because there are widespread increases in cloud cover (Fig. 6o), which may cause ET to become more energy-limited in agreement with Stéfanon et al. (2014). However, in regions where ET is moisture-limited, it can increase even though cloud cover has increased and SWnet, dominated by changes in downwelling surface shortwave radiation (SWdown) has decreased (Supplementary Figure 6i to l). Local and/or regional circulation changes are also possible but have not been investigated.

3.3.2 Impact of a change in runoff scheme

The change in runoff scheme in UM10.1 from PDM to TOPMODEL[6] results in significant increases in ET and decreases in 1.5 m temperature over much of the domain (Fig. 9b and c). Precipitation also increases in most areas (Fig. 9a) and there are small increases in cloud fraction (Fig. 9e), more negative SWnet and more positive LWnet at the surface (Supplementary Figure 9a and b). Dry precipitation biases are decreased over France and towards the east of the domain although there are increased wet biases in some areas such as the Alps contributing to an increase in RMSE (Fig. 10). Warm biases are decreased in the southeast of the domain with an overall decrease in RMSE (Fig. 11). Additional sensitivity tests over Europe (not shown) and similar tests over the UK (Bush et al., in prep.) showed that of the three settings (runoff, soil hydraulics, direction of movement of excess soil moisture), the change in runoff scheme is the main factor leading to the changes in precipitation and temperature. Focussing on mean values over France (Fig. 4: red and brown lines), the change results in decreased total runoff in autumn and winter and increased top layer soil moisture and ET in summer and the increase in ET occurs through soil as opposed to canopy evaporation. This sensitivity of ET to runoff scheme, especially when soil moisture is limited is in agreement with Gedney et al. (2000).

[6] This change is implemented in combination with the change in direction of movement of excess soil moisture from up to down and the change in soil hydraulic scheme from van Genuchten to Brooks-Corey (Table 1).

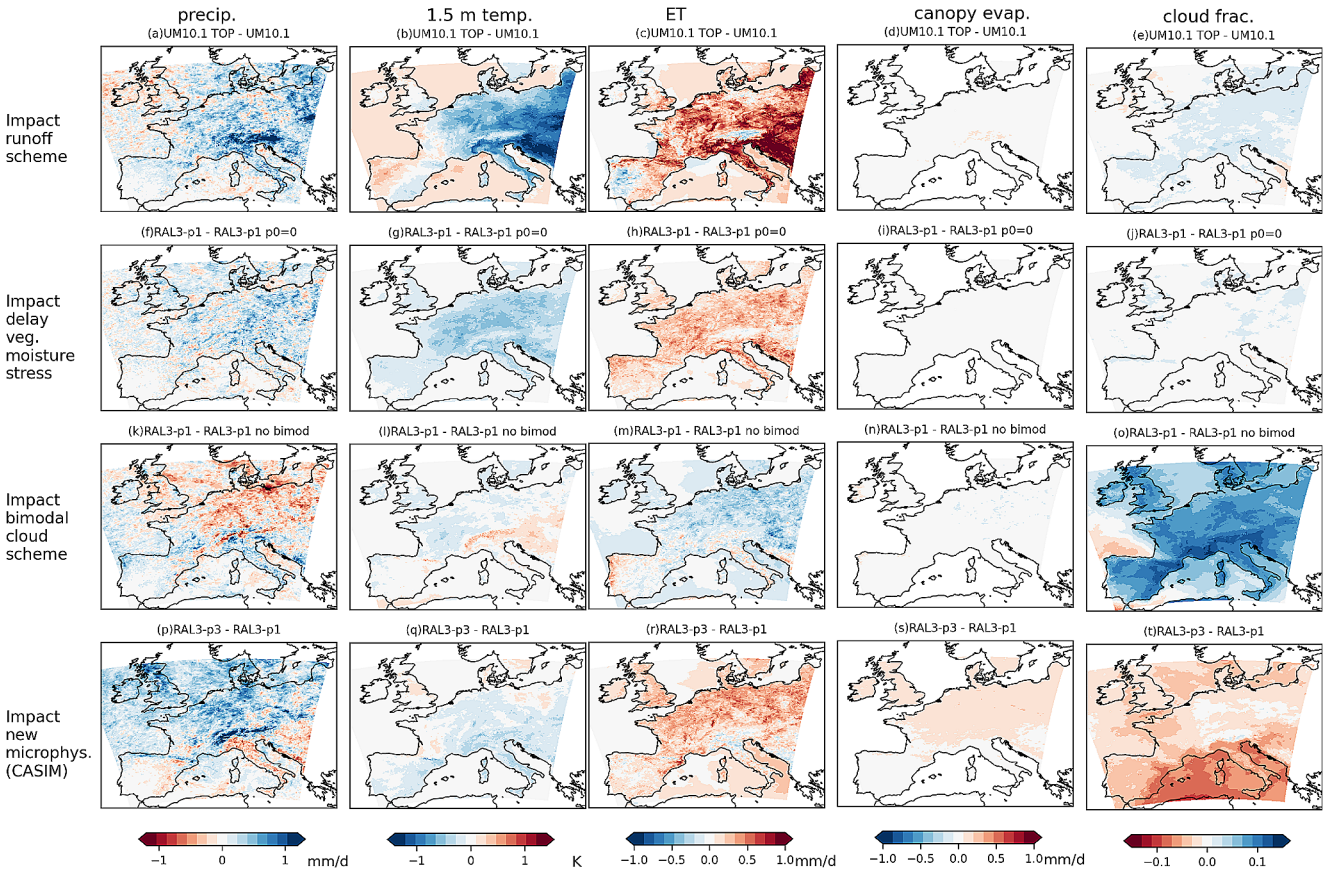

Fig. 9 Mean JJA difference (2000–2004) between standard UM10.1 and RAL3-p1 configurations and 5-year sensitivity tests. First row: UM10.1 with TOPMODEL, second row: RAL3-p1 with p0 = 0, third row: RAL3-p1 with no bimodal cloud scheme and fourth row: RAL3-p3 (includes CASIM microphysics scheme) for (a),(f),(k),(p) precipitation (mm/day), (b),(g),(l),(q) 1.5 m temperature (K), (c),(h),(m),(r) ET (mm/day), (d),(i),(n),(s) canopy evaporation (mm/day) and (e),(j),(o),(t) cloud fraction

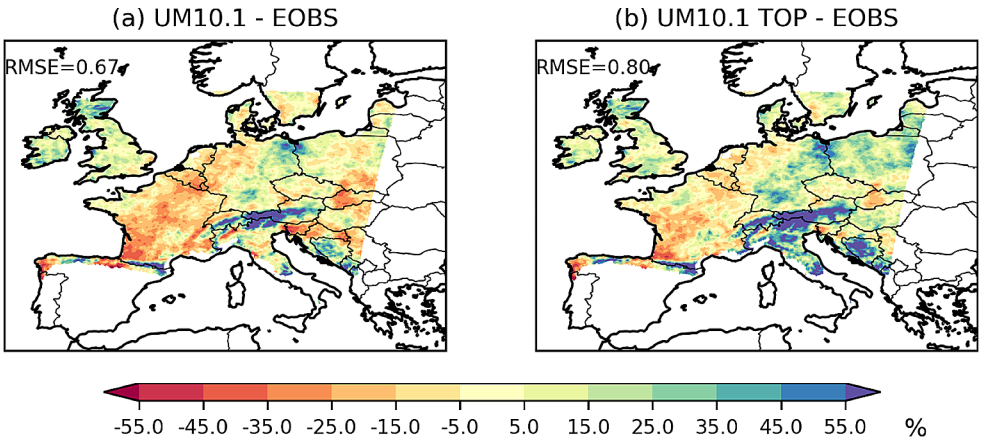

Fig. 10 JJA percent precipitation bias (2000–2004) and RMSE compared with observations from E-OBS for (a) UM10.1-original, (b) UM10.1 with TOPMODEL. Regions with mean precipitation of less than 1 mm per day during the period of evaluation are masked

3.3.3 The combined effect of the changes in soil properties, moisture stress threshold and cloud scheme

In all RAL3 simulations, we see lower moisture in all soil layers (Fig. 4: purple, yellow, blue and grey lines) compared with UM10.1 and the RCM. This also occurs in UK simulations with the same configuration (Bush et al., in prep.) and is the result of updated soil properties; however, ET stays relatively high due to the change in the p0 parameter which delays the onset of soil moisture limitation of transpiration. This acts to limit high 1.5 m temperatures by increasing the latent heat flux and reducing the sensible heat flux, for example, in the southeast UK (Bush et al., in prep.). The p0 change, which is part of all RAL3 configurations (i.e.

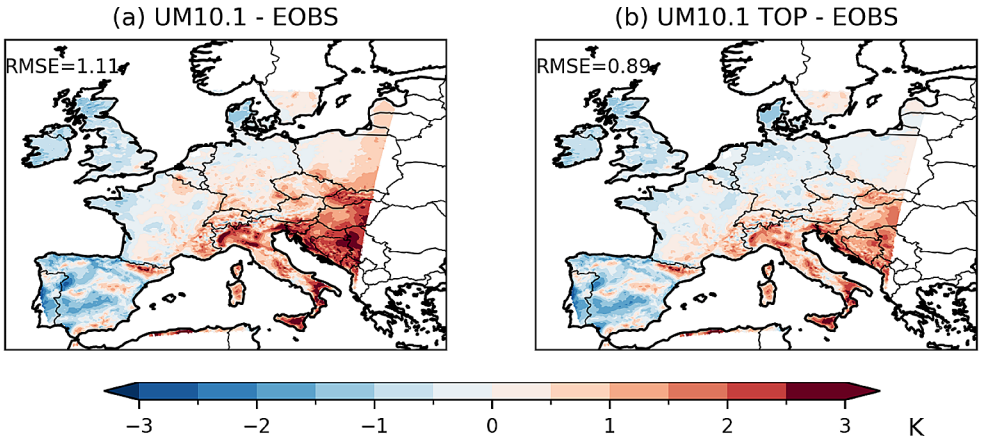

Fig. 11 JJA 1.5 m temperature bias (K) (2000–2004) and RMSE compared with observations from E-OBS for (a) UM10.1-original, (b) UM10.1 with TOPMODEL

p0 = 0.6 as opposed to 0.0) leads to widespread decreases in temperature, increases in ET and smaller increases in precipitation (Fig. 9f to j). However, the dry precipitation bias worsens in many areas in RAL3-p1 compared with UM10.1 (Fig. 1b and c), despite decreases in the ET bias (Fig. 3b and c). This may be explained at least in part by the use of the bimodal cloud scheme in RAL3, as shown in sensitivity tests (Fig. 9k to o) and in similar experiments for the UK (Bush et al., in prep.). This is discussed further in Sect. 3.4. Here we have shown that although the p0 change produces higher ET for a given soil moisture content, it is counteracted by other changes in the RAL3-p1 configuration.

3.4 Atmospheric processes

3.4.1 Impact of the change in cloud scheme

The bimodal cloud scheme leads to widespread increases in cloud fraction, more negative SWnet and decreased precipitation and ET over more northern areas (Figure 4k to o, Supplementary Figure 9i). Experiments over the UK showed that the bimodal cloud scheme is associated with less low cloud and more high cloud. Similar low cloud biases have also been linked to dry precipitation biases in RCM simulations by Bastin et al. (2018).

3.4.2 Impact of change in the microphysics scheme in relation to the precipitation intensity distribution and canopy evaporation

Changing the microphysics scheme from Wilson & Ballard (RAL3-p1) to CASIM (RAL3-p3) increases precipitation across northern areas (Fig. 9p). ET also increases in the same region (Fig. 9r), suggesting that CASIM results in increased recycling of local moisture. CASIM also decreases 1.5 m temperature in most areas (Fig. 9q). Cloud fraction decreases over most areas except the Alps and some areas in the north and east of the domain where it is unchanged (Fig. 9t). There are also large increases in SWdown and SWnet in northern parts of the domain, which is consistent with increased ET, and small decreases in LWdown and LWnet (Supplementary Figure 9m to p). These results suggest that the relationships between cloud fraction, radiation and precipitation and 1.5 m temperature have been altered by the change in microphysics scheme. The changes associated with the introduction of the CASIM microphysics scheme (RAL3-p3) (i.e. lower temperatures, higher ET, less cloud, increased SWdown and increased light and decreased heavy precipitation) are consistent with changes found in equivalent simulations performed for the UK and Africa in summer. Increased total precipitation in many areas was also found for the UK and Europe. These changes are mostly beneficial and act to reduce dry and warm biases and RMSE values compared to other CPM configurations (Figs. 1 and 2).

Although CPMs generally improve the precipitation intensity distribution, the heavier precipitation tends to be too intense in the older configurations (Berthou et al. 2020). The switch to CASIM shifts the precipitation intensity distribution back towards that of the RCMs i.e. there is more light and less heavy precipitation (Figure 12), This is also seen in results for the UK (Bush et al., in prep.). An impact of the change in precipitation distribution is that there is more canopy evaporation (Fig. 4: blue line and Fig. 10s), as the increased frequency/duration of precipitation (but not necessarily the total amount) increases the availability of moisture on the canopy as is also the case in RCMs with frequent, light rainfall.

3.5 Additional sensitivity tests

Additional sensitivity tests (as described in the Supplementary information) including updated IGBP land cover, removing subgrid rainfall variability, changes to TOPMODEL parameters relating to sub-surface hydrology, soil properties from SoilGrids and enhanced infiltration did not

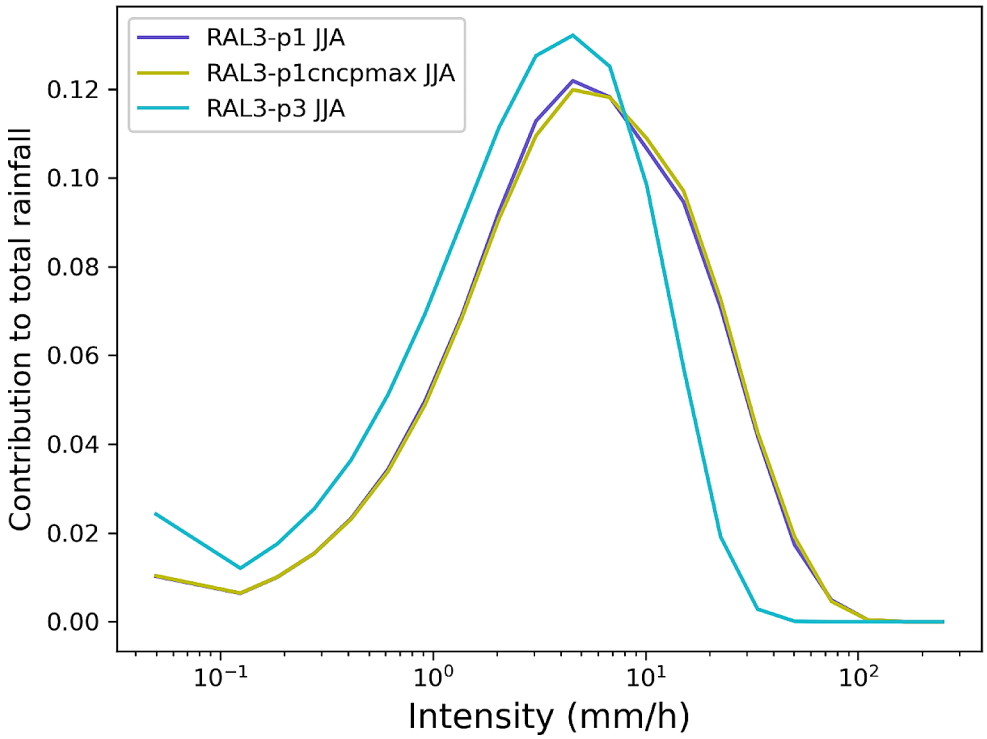

Fig. 12 JJA 1999 Precipitation intensity distribution based on hourly data over central France from RAL3-p1, RAL3-p1 with increased canopy capacity (RAL3-p1cncpmax) and RAL3-p3

have significant effects on precipitation or total ET (Supplementary Figure 12).

4 Summary and conclusions

In this study we have gained a better understanding of the summer precipitation and temperature biases in CPM simulations for Europe and the differences in the magnitude of these biases between CPM and RCM simulations. We have also tested alternative model configurations and setups such as increased soil moisture and canopy capacity to investigate the source of these biases. Our sensitivity tests show the following key results which are also summarised in Fig. 13:

- Using a more complex runoff scheme (TOPMODEL) that takes into account topography and represents the water table leads to improvements in warm and dry biases.
- When using the same runoff model, ET differences between RCM and CPM are dominated by differences in canopy evaporation (i.e. intercepted water) as opposed to evaporation from soil (including transpiration). This is explained by the modified precipitation intensity distribution.
- Large increases in the capacity of vegetation to intercept rainfall have a modest cooling effect but have very little impact on precipitation, suggesting that a larger, 'slower' soil or surface store is needed.
- Changing the microphysics scheme to a new double-moment scheme shifts the precipitation intensity distribution towards more light and less heavy precipitation, which can decrease warm biases by altering land surface feedbacks.
- Removing soil moisture deficits in southern Europe can eliminate dry precipitation biases via a positive soil-moisture precipitation feedback.
- TOPMODEL and delayed onset of moisture stress in vegetation (which increases transpiration) decrease warm/dry biases. In RAL3 configurations, these changes are counteracted by the bimodal cloud scheme, resulting in increased biases when these changes are combined.

We have seen that increasing soil moisture in the top layers can eliminate dry precipitation biases in many areas by increasing ET and those areas are broadly consistent with negative ET biases. We suggest that increasing ET through soil evaporation (including transpiration) in southern Europe could both increase the dependence on 'slow' as opposed to 'fast' storage so that it is more consistent with observations and decrease the negative ET and precipitation biases. We note that areas with a negative ET bias and warm bias in the south and east (Figs. 2 and 3) correspond to areas with shallow water table depth in Figure 9 from Fan et al. (2013). Barlage et al. (2021) showed that in areas of the US with a shallow water table, warm biases were alleviated by using a groundwater scheme permitting lateral flows, two-way interactions with rivers and upward transport of moisture

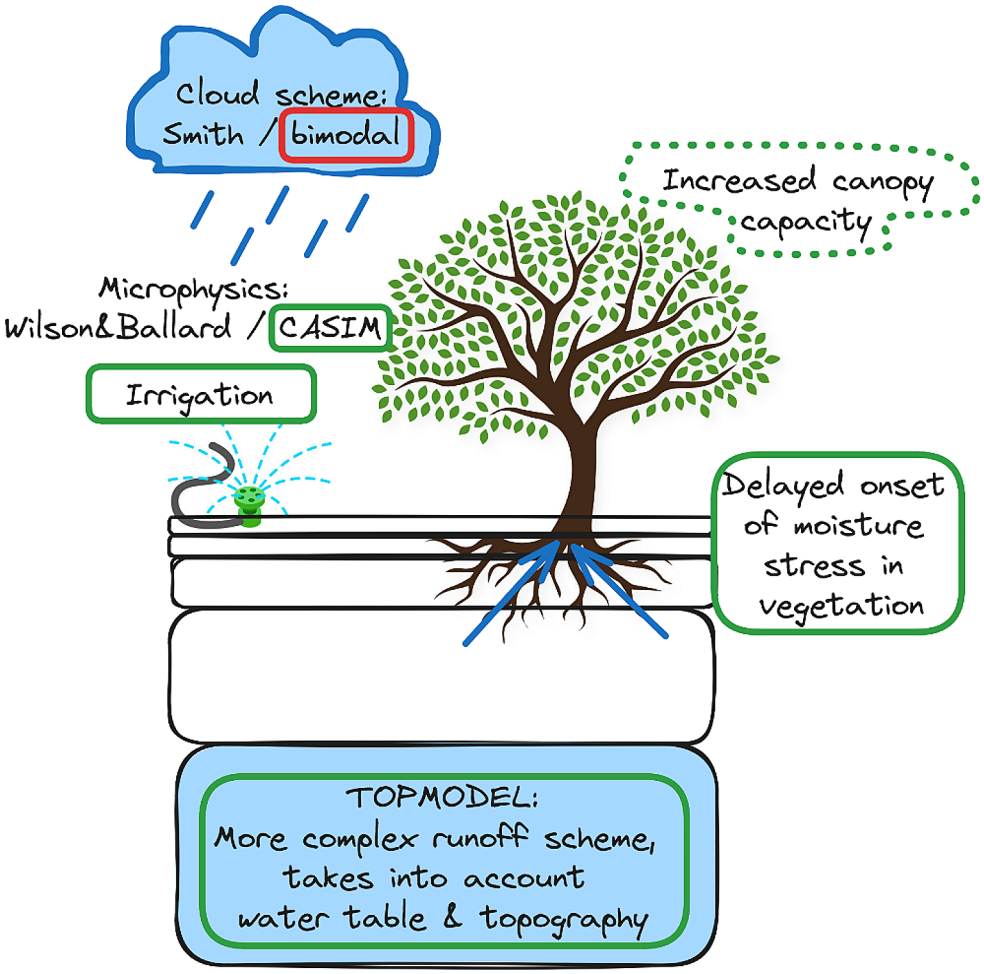

Fig. 13 Schematic diagram illustrating the sensitivity tests listed in Table 1. Green boxes indicate changes that decreased the dry or warm biases, dashed green boxes indicate changes that had minimal impact and red boxes indicate changes that increased biases

from the deep layer to the soil column. Importantly, this scheme showed increased benefits at high spatial resolution. Though the simulations were not convection-permitting, Martinez et al. (2016) showed that dry season soil moisture, ET and downstream precipitation could be increased by adding a groundwater scheme. This suggests that addition of such a scheme may alleviate temperature and ET biases by increasing moisture availability for evaporation/transpiration. Other ways to increase moisture in the soil store include increasing the depth of the lowest soil layer (which has been tested in JULES but not at high resolution in the UM), a surface pooling scheme to increase the surface store and slow infiltration, implementation of a realistic irrigation scheme (Boone et al. 2021; Brooke et al. 2024). In future work, we would like to explore: (1) spatially varying values of decay of hydraulic conductivity with depth in TOPMODEL depending on bedrock properties as opposed to using fixed values, (2) sensitivity of precipitation to increased soil moisture in a future climate scenario to assess whether regions that are soil-moisture limited increase in spatial extent and (3) combining SoilGrids soil parameters with different pedotransfer functions from Zhang and Schaap (2017) and van Genuchten soil hydraulics, which has been shown to increase soil moisture and decrease summer temperatures in the UM at lower resolution (P. McGuire, pers. comm.).

Although we have used the UM for our experiments, it is likely that many of our results are applicable to other regions where convection-permitting models are affected by warm and dry biases, not least because other CPMs tend to exhibit similar changes in the nature of precipitation compared to traditional coarser resolution climate models. In relation to the cause of the biases, we conclude that the land surface scheme currently employed has not been designed for use with the different nature of rainfall at km-scales; rainfall rates are too high for the canopy to intercept a significant proportion (even when capacity is increased) or for rainfall to infiltrate the soils. Therefore, a key longer-term challenge for land surface schemes in high resolution CPMs is that as model resolution increases and the nature of rainfall is more intense and intermittent, additional complexity and restructuring is required in order to take into account processes (e.g. horizontal groundwater transport, Barlage et al. 2021) that were previously neglected or less important at

lower resolution. Including these processes is recommended with a view to increasing the reliability of land surface feedbacks and hence future climate projections. Here we are only beginning to address these challenges, though we have taken practical steps to find better solutions whilst advancing our knowledge of land surface behaviour in CPMs.

Supplementary Information The online version contains supplementary material available at https://doi.org/10.1007/s00382-024-07192-4.

Acknowledgements We thank Chris Short and Simon Tucker for technical assistance and Adrian Lock for useful discussions. We acknowledge the E-OBS dataset from the EU-FP6 project UERRA (http://www.uerra.eu) and the data providers in the ECA&D project (https://www.ecad.eu).

Author contributions All authors contributed to the study conception and design. Model simulations were performed by Kate Halladay, Ségolène Berthou and Elizabeth Kendon. Figures 1, 2, 3, 4, 5, 6, 7, 8, 9, 10, 11 and 12 and supplementary figures were prepared by Kate Halladay and Figure 13 by Ségolène Berthou. The first draft of the manuscript was written by Kate Halladay, Ségolène Berthou and Elizabeth Kendon and all authors commented on previous versions of the manuscript. All authors read and approved the final manuscript.

Funding This study received support from the European Union's Horizon 2020 EUCP project (Grant No. GA776613) and from the Joint UK BEIS/Defra Met Office Hadley Centre Climate Programme (Grant No. GA01101).

Data availability The Unified Model data analysed during the current study are available from the corresponding author on reasonable request.

Declarations

Ethics approval and consent to participate Not applicable.

Consent for publication Not applicable.

Competing interests The authors declare no competing interests.

References

Barlage M, Chen F, Rasmussen R, Zhang Z, Miguez-Macho G (2021) The importance of scale-dependent groundwater processes in land-atmosphere interactions over the central United States. Geophys Res Lett, 48(5), e2020GL092171.

Bastin S, Chiriaco M, Drobinski P (2018) Control of radiation and evaporation on temperature variability in a WRF regional climate simulation: comparison with co-located long term ground-based observations near Paris. Clim Dyn 51(3):985–1003

Berthou S, Kendon EJ, Chan SC, Ban N, Leutwyler D, Schär C, Fosser G (2020) Pan-european climate at convection-permitting scale: a model intercomparison study. Clim Dyn 55(1):35–59

Best MJ, Pryor M, Clark DB, Rooney GG, Essery R, Ménard CB et al (2011) The Joint UK Land Environment Simulator (JULES), model description–part 1: energy and water fluxes. Geosci Model Dev 4(3):677–699

Boone A, Bellvert J, Best M, Brooke J, Canut-Rocafort G, Cuxart J, Hartogensis O, Le Moigne P, Miró J, Polcher J, Price J, Quintana Seguí J, Wooster M (2021) Updates on the international land surface interactions with the atmosphere over the Iberian Semi-arid Environment (LIAISE) Field Campaign. Gewex News 31(4):17–21

Breuer L, Eckhardt K, Frede HG (2003) Plant parameter values for models in temperate climates. Ecol Model 169(2–3):237–293

Brooke JK et al (2024) Irrigation contrasts through the morning transition. Quart J Royal Meteorol Soc 150(758):170–194

Brooks RH, Corey AT (1964) Hydraulic properties of porous media, Hydrological Papers 3, Colorado State Univ., Fort Collins

Bush M, Allen T, Bain C, Boutle I, Edwards J, Finnenkoetter A, Franklin C, Hanley K, Lean H, Lock A et al (2020) The first Met Office Unified Model–JULES Regional Atmosphere and Land configuration, RAL1, Geosci. Model Dev 13:1999–2029. https://doi.org/10.5194/gmd-13-1999-2020

Bush M, Flack D, Arnold A, Best M et al Unifying Mid-latitude and Tropical Regional Model 3 Configurations: The third Met Office Unified 4 Model–JULES Regional Atmosphere and Land 5 Configuration, RAL3. In preparation for QJRMS

Davies-Barnard T, Valdes PJ, Jones CD, Singarayer JS (2014) Sensitivity of a coupled climate model to canopy interception capacity. Clim Dyn 42(7):1715–1732

Denissen JM, Teuling AJ, Reichstein M, Orth R (2020) Critical soil moisture derived from satellite observations over Europe. J Geophys Research: Atmos, 125(6), e2019JD031672.

Dong J, Lei F, Crow WT (2022) Land transpiration-evaporation partitioning errors responsible for modeled summertime warm bias in the central United States. Nat Commun 13(1):1–8

Fan Y, Li H, Miguez-Macho G (2013) Global patterns of groundwater table depth. Science 339(6122):940–943

Field P, Hill A, Shipway B et al (2023) Implementation of a double moment cloud microphysics in UK Met Office regional Numerical Weather Prediction. QJRMS 149(752):703–739

Folwell SS, Taylor CM, Stratton RA (2022) Contrasting contributions of surface hydrological pathways in convection permitting and parameterised climate simulations over Africa and their feedbacks on the atmosphere. Clim Dyn, 1–16

Gedney N, Cox PM (2003) The sensitivity of global climate model simulations to the representation of soil moisture heterogeneity. J Hydrometeorol 4(6):1265–1275

Gedney N, Cox PM, Douville H, Polcher J, Valdes PJ (2000) Characterizing GCM land surface schemes to understand their responses to climate change. J Clim 13(17):3066–3079

Guillod BP, Orlowsky B, Miralles DG, Teuling AJ, Seneviratne SI (2015) Reconciling spatial and temporal soil moisture effects on afternoon rainfall. Nat Commun 6(1):6443

Guo Z, Dirmeyer PA, Koster RD, Sud YC, Bonan G, Oleson KW et al (2006) GLACE: the global land–atmosphere coupling experiment. Part II: analysis. J Hydrometeorol 7(4):611–625. https://doi.org/10.1175/JHM511.1

Halladay K, Kahana R, Johnson B, Still C, Fosser G, Alves L (2023) Convection-permitting climate simulations for South America with the Met Office Unified Model. Climate Dynamics, pp 1–23

Harper AB, Williams KE, McGuire PC, Duran Rojas MC, Hemming D, Verhoef A et al (2021) Improvement of modeling plant responses to low soil moisture in JULESvn4. 9 and evaluation against flux tower measurements. Geosci Model Dev 14(6):3269–3294

Hartley AJ, MacBean N, Georgievski G, Bontemps S (2017) Uncertainty in plant functional type distributions and its impact on land surface models. Remote Sens Environ 203:71–89

Hengl T, Mendes de Jesus J, Heuvelink GB, Ruiperez Gonzalez M, Kilibarda M, Blagotić A et al (2017) SoilGrids250m: global gridded soil information based on machine learning. PLoS ONE, 12(2), e0169748

Hohenegger C, Brockhaus P, Bretherton CS, Schär C (2009) The soil moisture–precipitation feedback in simulations with explicit and parameterized convection. J Clim 22(19):5003–5020

Jung M, Koirala S, Weber U, Ichii K, Gans F, Camps-Valls G et al (2019) The FLUXCOM ensemble of global land-atmosphere energy fluxes. Sci data 6(1):74

Kendon EJ, Prein AF, Senior CA, Stirling A (2021) Challenges and outlook for convection-permitting climate modelling. Philosophical Trans Royal Soc A 379(2195):20190547

Klein C, M Taylor C (2020) Dry soils can intensify mesoscale convective systems. Proc Natl Acad Sci 117(35):21132–21137

Leutwyler D, Imamovic A, Schär C (2021) The continental-scale soil moisture–precipitation feedback in Europe with parameterized and explicit convection. J Clim 34(13):5303–5320

Loveland TR, Reed BC, Brown JF, Ohlen DO, Zhu Z, Yang LWM, Merchant JW (2000) Development of a global land cover characteristics database and IGBP DISCover from 1 km AVHRR data. Int J Remote Sens 21(6–7):1303–1330

Martens B, Miralles DG, van der Lievens H, de Jeu RAM, Fernández-Prieto D, Beck HE, Dorigo WA, Verhoest, N E C (2017) GLEAM v3: satellite-based land evaporation and root-zone soil moisture. Geosci Model Dev 10:1903–1925. https://doi.org/10.5194/gmd-10-1903-2017

Martinez JA, Dominguez F, Miguez-Macho G (2016) Impacts of a groundwater scheme on hydroclimatological conditions over southern South America. J Hydrometeorol 17(11):2959–2978

Miralles DG, Holmes TRH, De Jeu RAM, Gash JH, Meesters A, G C A, Dolman AJ (2011) Global land-surface evaporation estimated from satellite-based observations. Hydrol Earth Syst Sci 15(2):453–469

Moore RJ (1985) The probability-distributed principle and runoff production at point and basin scales. Hydrol Sci J 30(2):273–297

Reynolds RW, Smith TM, Liu C, Chelton DB, Casey KS, Schlax MG (2007) Daily high-resolution-blended analyses for sea surface temperature. J Clim 20(22):5473–5496

Smith RNB (1990) A scheme for predicting layer clouds and their water content in a general circulation model. Q J R Meteorol Soc 116(492):435–460

Stéfanon M, Drobinski P, D'Andrea F, Lebeaupin-Brossier C, Bastin S (2014) Soil moisture-temperature feedbacks at meso-scale during summer heat waves over Western Europe. Clim Dyn 42(5):1309–1324

Stratton RA, Senior CA, Vosper SB, Folwell SS, Boutle IA, Earnshaw PD et al (2018) A pan-african convection-permitting regional climate simulation with the Met Office unified model: CP4-Africa. J Clim 31(9):3485–3508

van der Cornes RC, Jones PD (2018) An ensemble version of the E-OBS temperature and precipitation data sets. J Geophys Research: Atmos 123(17):9391–9409

van Genuchten MT (1980) A closed-form equation for predicting the hydraulic conductivity of unsaturated soils. Soil Sci Soc Am J 44:892–898

Van Weverberg K, Morcrette CJ, Boutle I, Furtado K, Field PR (2021) A bimodal diagnostic cloud fraction parameterization. Part I: motivating analysis and scheme description. Mon Weather Rev 149(3):841–857

Zhang Y, Schaap MG (2017) Weighted recalibration of the Rosetta pedotransfer model with improved estimates of hydraulic parameter distributions and summary statistics (Rosetta3). J Hydrol 547:39–53